FUSION TECHNOLOGY

Annual Report of the Association EURATOM/CEA 2002

Compiled by : Ph. MAGAUD and F. Le VAGUERES

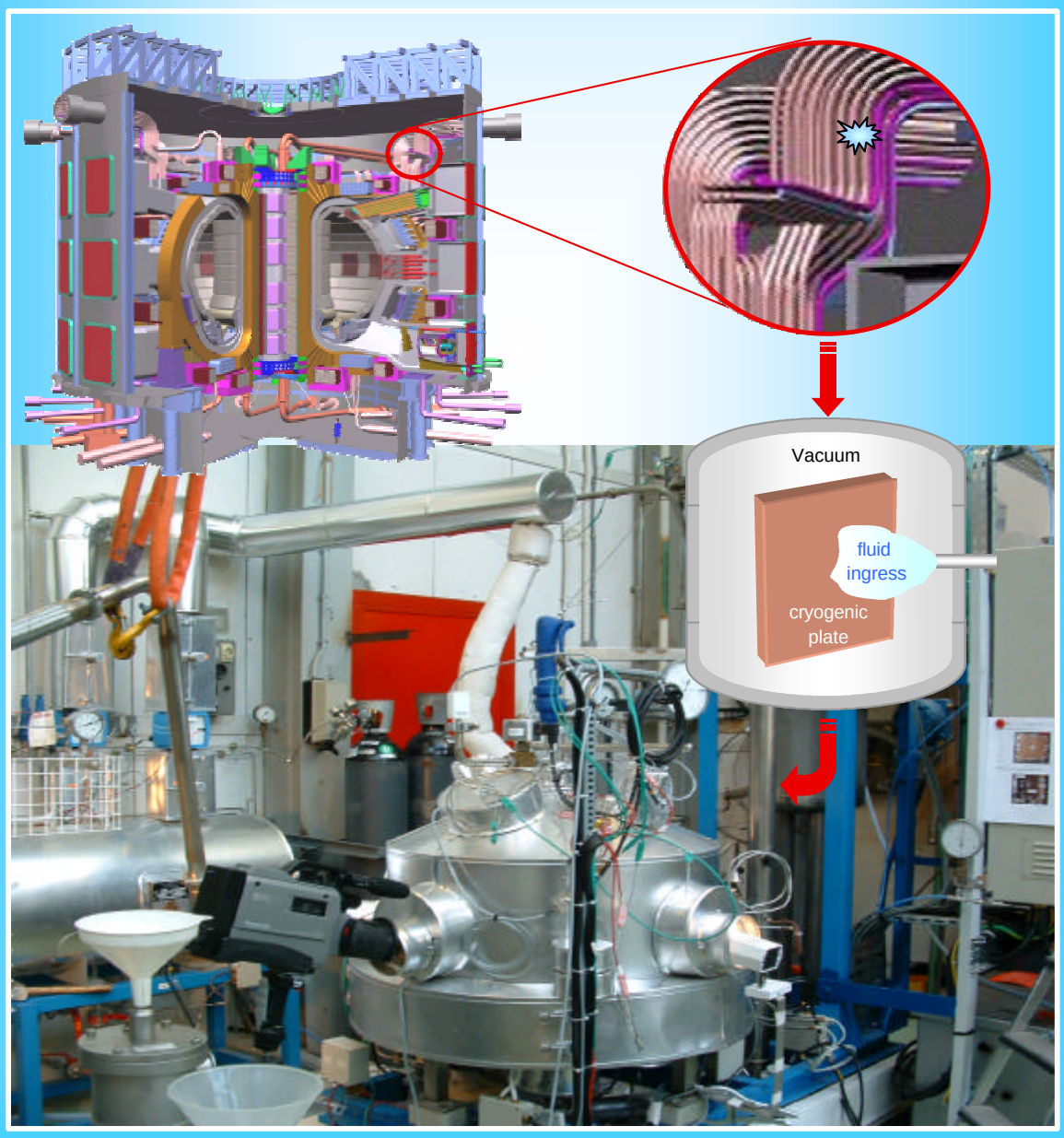

ASSOCIATION EURATOM/CEA
DSM/DRFC
CEA/CADARACHE
13108 Saint-Paul-Lez-Durance (France)

CONTENTS

Plasma Facing Components

Remote Handling

Magnet Structure

Tritium Breeding and Materials

Breeding Blanket

Water Cooled Lithium Lead (WCLL) blanket

Helium Cooled Pebble Bed (HCPB) blanket

Helium Cooled Lithium Lead (HCLL) blanket

Structural materials development

Reduced Activation Ferritic Martensitic (RAFM) steels

System Studies

Power Plant Conceptual Studies (PPCS)

Socio-economic studies

JET Technology

Physics Integration

Diagnostics

Vessel/In-Vessel

Plasma Facing Components

Remote Handling

Safety and Environment

UNDERLYING TECHNOLOGY PROGRAMME 315

Physics Integration

Diagnostics

Vessel/In-Vessel

Plasma Facing Components

Remote Handling

Tritium Breeding and Materials

Breeding Blanket

Materials development

Structural materials

Fuel cycle

Safety and Environment

System studies

INERTIAL CONFINEMENT FUSION PROGRAMME 413

SEA5-31

Task Title: VALIDATION OF COMPUTER CODES AND MODELS

INTRODUCTION

The overall objective is to improve the validation level of the computer codes, which are used for the safety assessment of ITER.

In this frame, The scope of the fusion thermalhydraulic codes benchmark is to assess the capabilities of best estimate thermal hydraulic codes to simulate the main physical phenomena occurring during an in-vessel break transient within a water-cooled fusion-type reactor: pressurisation of a volume at low initial pressure, critical flow, counter pressure effect, relief into an expansion volume.

Several cases have been treated which were specific to one particular phenomenon. An additional case has been defined which refers to ITER operating conditions.

2002 ACTIVITIES

A sketch of the configuration is presented on the figure 1 on which the initial conditions are reported. The opening thresholds of the valves is also mentioned.

The main components which are taken into account are the pressurised water Cooling Loop (CL), whose function is to extract the nuclear power, the Plasma Chamber (PC) where the fusion reactions occur, the Drain Tank (DT) whose function is to receive the final products (liquid water) of a break of the CL, the Suppression Tank (ST) whose function is to cut off the overpressure in the PC ; a Distributor (DIS) is placed between PC and ST to increase the condensation of the steam inside the ST.

These components are connected by pipes supposed to be thermally insulated for steam and water circulation.

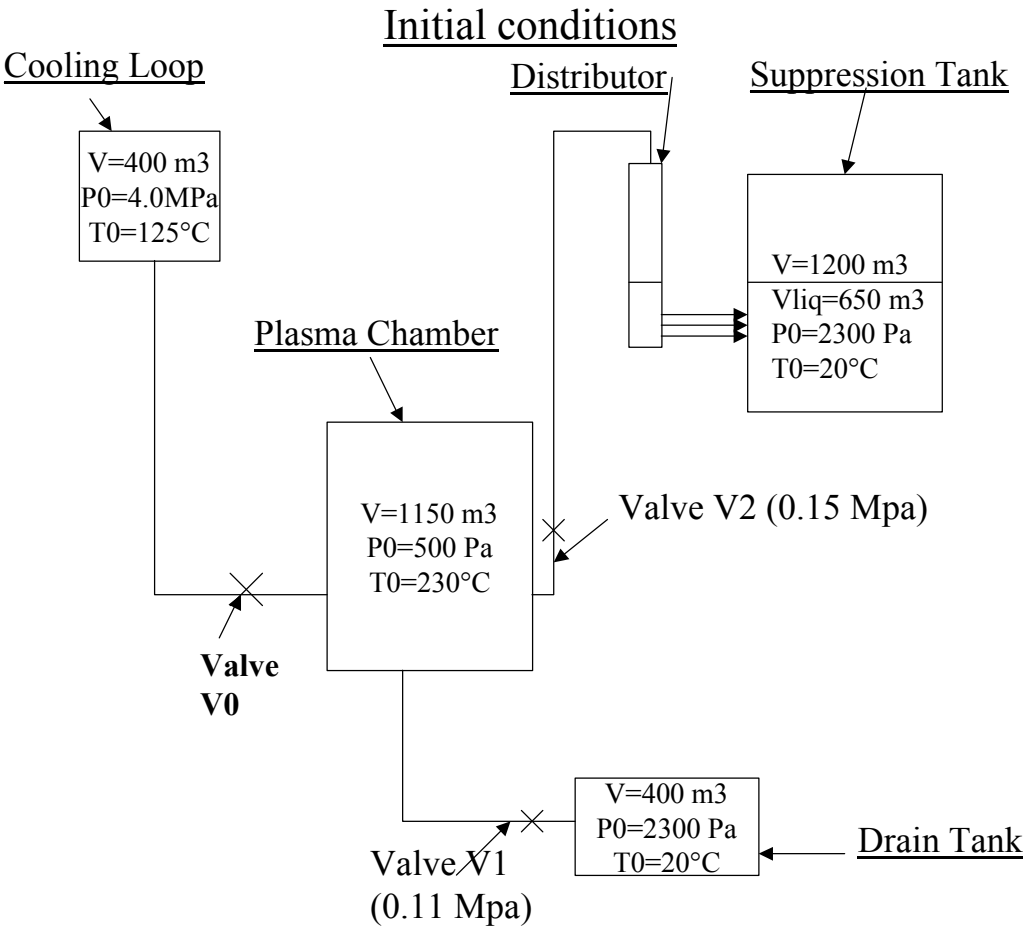

Figure 1 : Fusion codes benchmark – ITER case

The main characteristics of the codes involved in this case as summurized in the following table:

Code	Physical model	Critical flow model
CATHARE	6 equations non equilibrium	Derived from the basic TH model
MELCOR	6 equations non equilibrium	Sub cooled: Henry Fauske Saturated: Moody Vapour: Ideal gas isentropic expansion
RELAP	6 equations non equilibrium	Two-phase choking criterion (Ransom) Sub cooled: empirical correlation
CONSEN	Homogeneous equilibrium	G2=F(P,ν,X) Gas: G2 = F(P,ρ,γ)

The main results are shown on the figures 2 and 3. All codes predict that the pressure peak within the plasma chamber is lower than the design pressure (2 MPa). Thanks to the condensation of the steam in the suppression tank, the pressure is stabilized at a relatively low value at the end of the transient (figure 2).

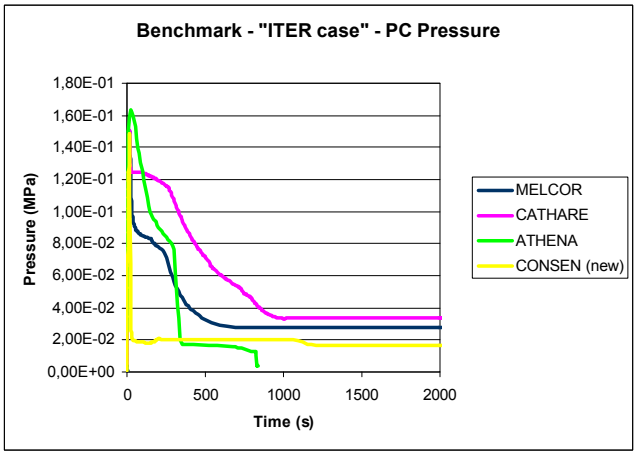

Figure 2 : Pressure evolution within the plasma chamber

Discrepancies are observed concerning the break mass flow rate, which are due to the different critical flow models implemented in the codes (figure 3).

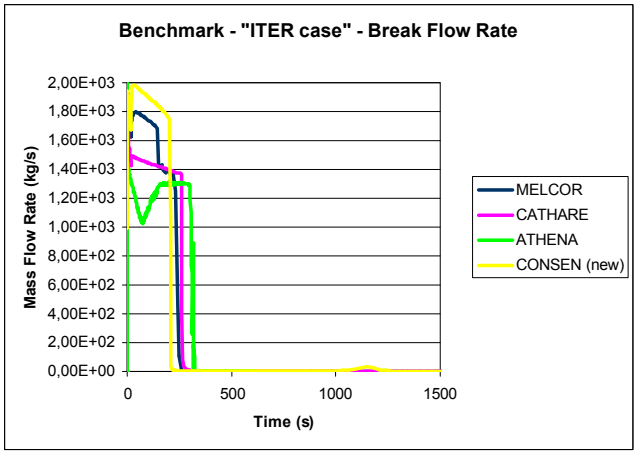

Figure 3 : Evolution of the break mass flow rate

CONCLUSIONS

The results which are given by the codes in the frame of this benchmark are of the same order of magnitude. However discrepancies have been observed which are mainly due to the different ways the codes calculate the break mass flow rate and the pressurisation of the vacuum vessel. The calculation of a whole accidental sequence requires an accurate simulation of the physical phenomena in order to obtain low uncertainties on the results. For each accidental sequence to be treated, it must be checked if the physical model of the code which will be used are suitable for the expected flow conditions.

REPORTS AND PUBLICATIONS

P. Sardain, Synthesis of the fusion codes benchmark, CEA Report SERI/LFEA 03/50XX, to be issued.

TASK LEADER

Pierre SARDAIN

DER/SERI/LFEA
CEA Cadarache
13108 Saint Paul Lez Durance Cedex

Tél. : 33 4 42 25 37 59
Fax : 33 4 42 25 36 35

E-mail : pierre.sardain@cea.fr

TW1-TSS-SEA5

Task Title: VALIDATION OF COMPUTER CODES AND MODELS

INTRODUCTION

In the frame of the validation of the computer codes which are used for the assessment of ITER safety, the EVITA experiment allow to simulate the physical phenomena occurring during a coolant ingress into the vacuum vessel and the cryostat. The main experimental results are the pressure within the vessel, the temperatures of the structures, the amount of ice formed on the cryogenic surface.

2002 ACTIVITIES

A sketch of the EVITA experiment is given in the figure 1. Water or steam can be injected from the pressurizer into the vacuum vessel. The cryogenic plate, which is located inside the vacuum vessel is cooled by nitrogen at 80 K; its total surface is 0.1 m^2.

Two series of cryogenic tests have been performed: the "cryogenic condensation" tests in which all the injected power is removed by the cryogenic plate and the "cryogenic pressurization" tests in which the cryogenic plate does not remove all the injected power.

The main data of the tests are the initial pressure and temperature of the injected fluid, the injection mass flow rate, the initial temperatures of the internal structures and the operating conditions inside the nitrogen loop.

In most tests fluxmeters have been implemented on one face of the cryogenic plate.

No stable ice layer on the cryogenic plate has been obtained when the fluxmeters were removed.

The fluxmeters probably act as thermal protection, limiting the temperature increase of the cryogenic plate.

The average mass of the stable ice layer, when obtained, was about 300 g.

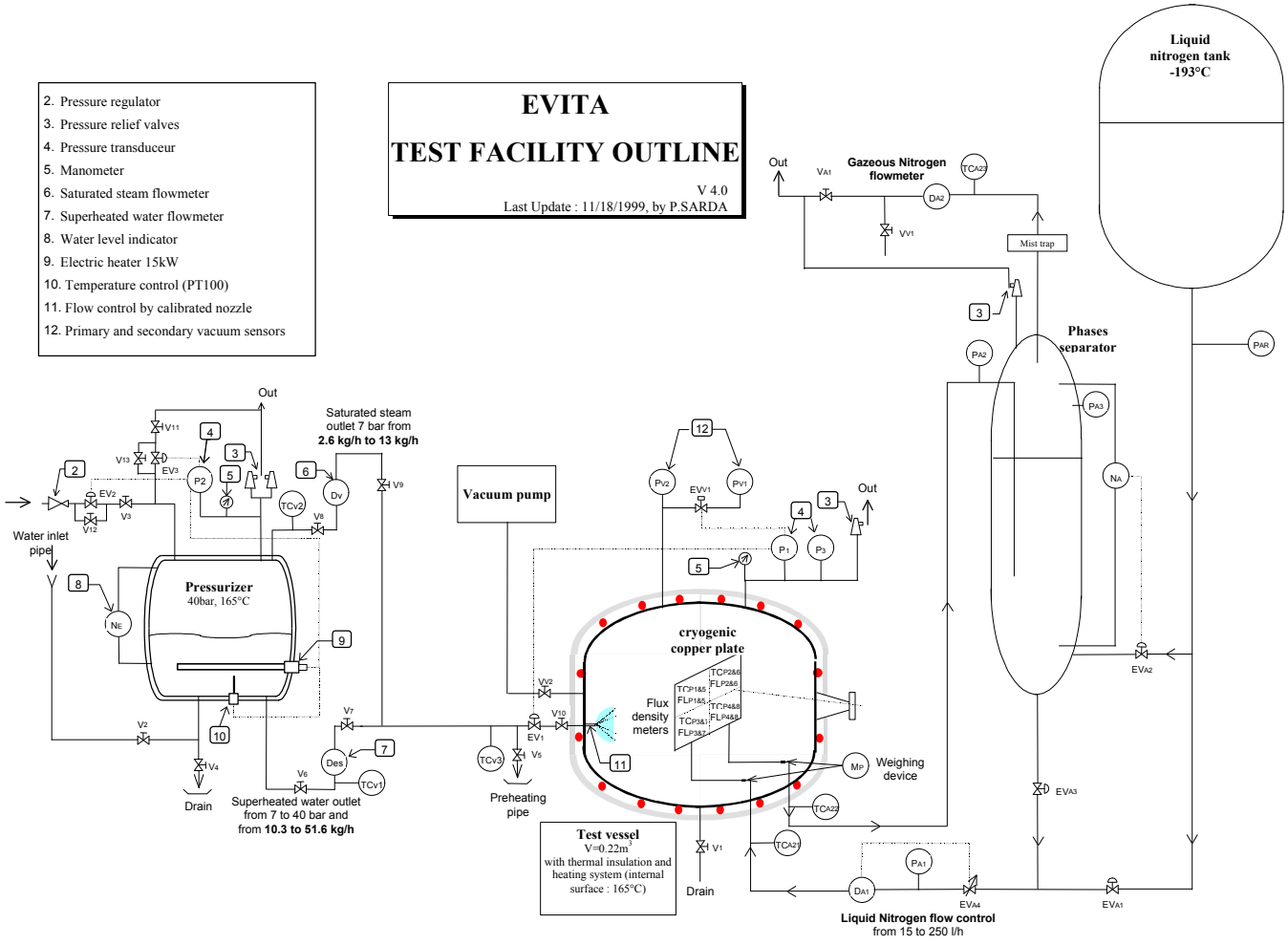

Figure 1 : Sketch of the EVITA experiment

The cryogenic tests have been calculated using the PAXITR computer code. PAXITR is a 0D code which is mainly used to evaluate the depressurisation of a containment and the resulting pressurisation of a vessel receiving the fluid from the depressurisation. The PAXITR modelling is shown on the figure 2. The model includes internal structure representing the wet wall and the dry wall of the vessel, the jet impingement area and the cryogenic plate.

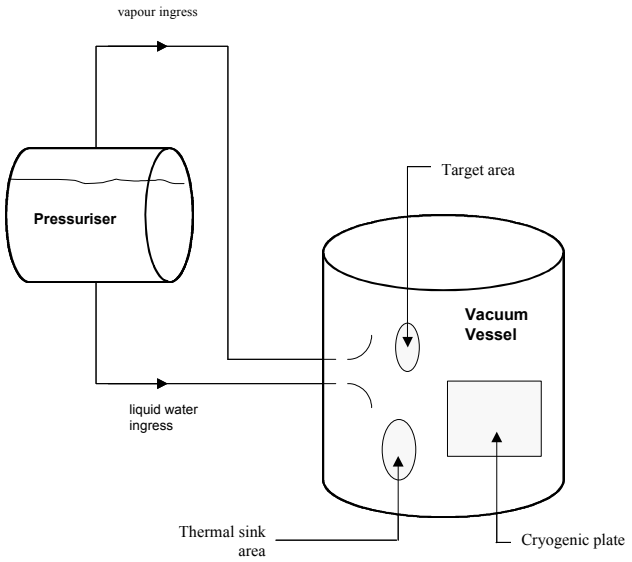

Figure 2 : PAXITR modelling for EVITA

A comparison of experimental results and PAXITR calculation is shown on the figure 3. It concerns a "cryogenic condensation" test in which the initial temperature of the walls of the vessel was 25°C. The pressure and temperature of the injected water were respectively 4 MPa and 165°C.

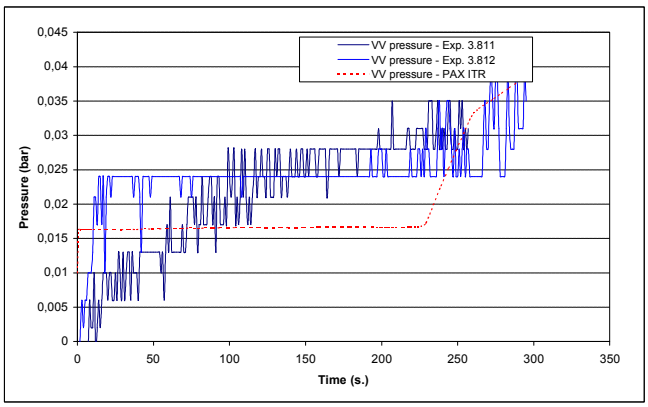

Figure 3 : Comparison experiment/calculation

CONCLUSIONS

The EVITA programme has provided results which can be used for the validation of the computer codes. It notably allows to improve the cryogenic models.

REPORTS AND PUBLICATIONS

S. Sellier et al. , first experimental results of EVITA cryogenic tests, CEA report STR/LCET 02/033

L.B. Marie, EVITA PXITR2 – second set of calculations – cryogenic condensation tests and cryogenic pressurisation tests, TA – 284722 / A

TASK LEADER

Pierre SARDAIN

DER/SERI/LFEA
CEA Cadarache
13108 Saint Paul Lez Durance Cedex

Tél. : 33 4 42 25 37 59
Fax : 33 4 42 25 36 35

E-mail : pierre.sardain@cea.fr

TW0-SEA3.5
TW1-TSS-SEA3.5

Task Title: IN-VESSEL HYDROGEN DEFLAGRATION/DETONATION ANALYSIS

INTRODUCTION

The scope of this study is to determine the hydrogen distribution within the ITER vacuum vessel during an in-vessel LOCA (loss of coolant accident) using a 3-D model.

The hydrogen comes from the chemical reaction between the steam and the beryllium. If the in-vessel LOCA is induced by an ex-vessel LOCA, an air ingress can occur, which is likely to lead to deflagration/detonation conditions.

2002 ACTIVITIES

The hydrogen distribution is calculated using the CAST3M code, which is a general multi-dimensional computational tool developed by CEA or structural mechanics, fluid dynamics, heat transfer and electromagnetism analysis.

An implicit finite element method is chosen for the discretization of the multi-component Navier-Stockes equations which govern the flow. Linear finite elements on hexahedra have been used, which are second order accurate in space.

A reaction rate model, function of the pressure and the first wall temperature, has been included in the code. Some initial and boundary conditions (wall temperatures, …) are provided by lumped-parameters calculations.

Since the code can not treat vacuum, a small quantity of air inside the vacuum vessel is assumed at the beginning of the transient.

As shown on the figure 1, two 3D meshes of the vacuum vessel have been done, one without port and one with the upper ports.

The hot wall is in red, the cold wall in blue and the break in green.

The figure 2 shows the hydrogen volume fractions within the vacuum vessel before the air ingress.

Two calculations have been made to check the influence of the upper port. It is shown that hydrogen tends to move upwards and accumulate.

After the air ingress, the maximum hydrogen concentration is higher when the upper ports are modelled. This shows that the upper ports must be considered in the geometrical model in order to obtain conservative results.

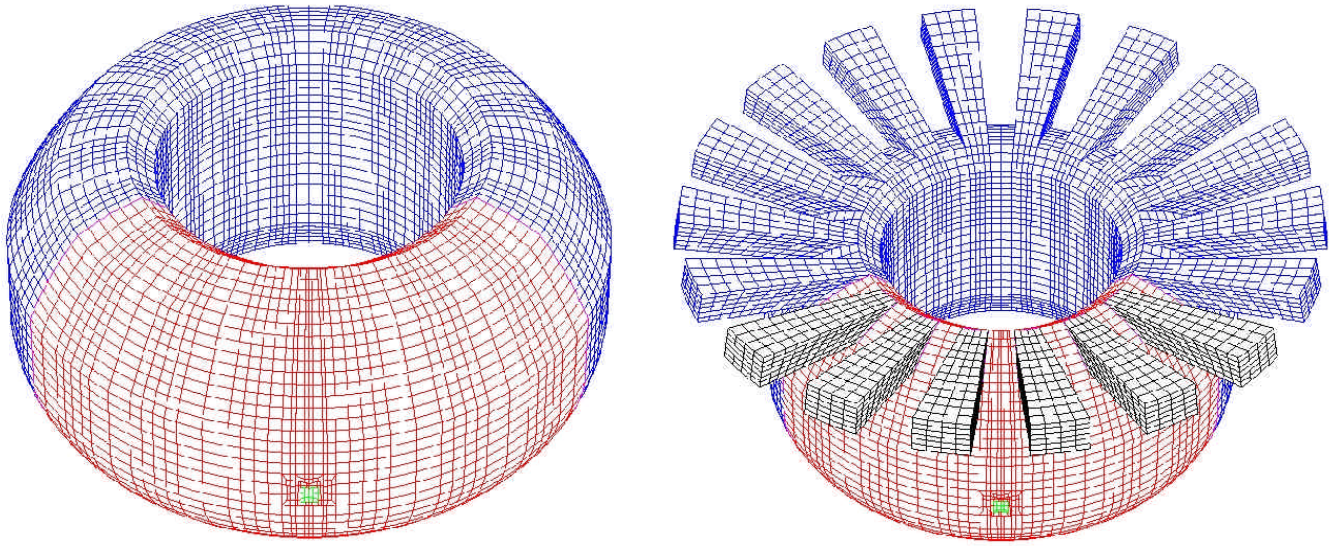

Figure 1 : 3D meshes of ITER vacuum vessel

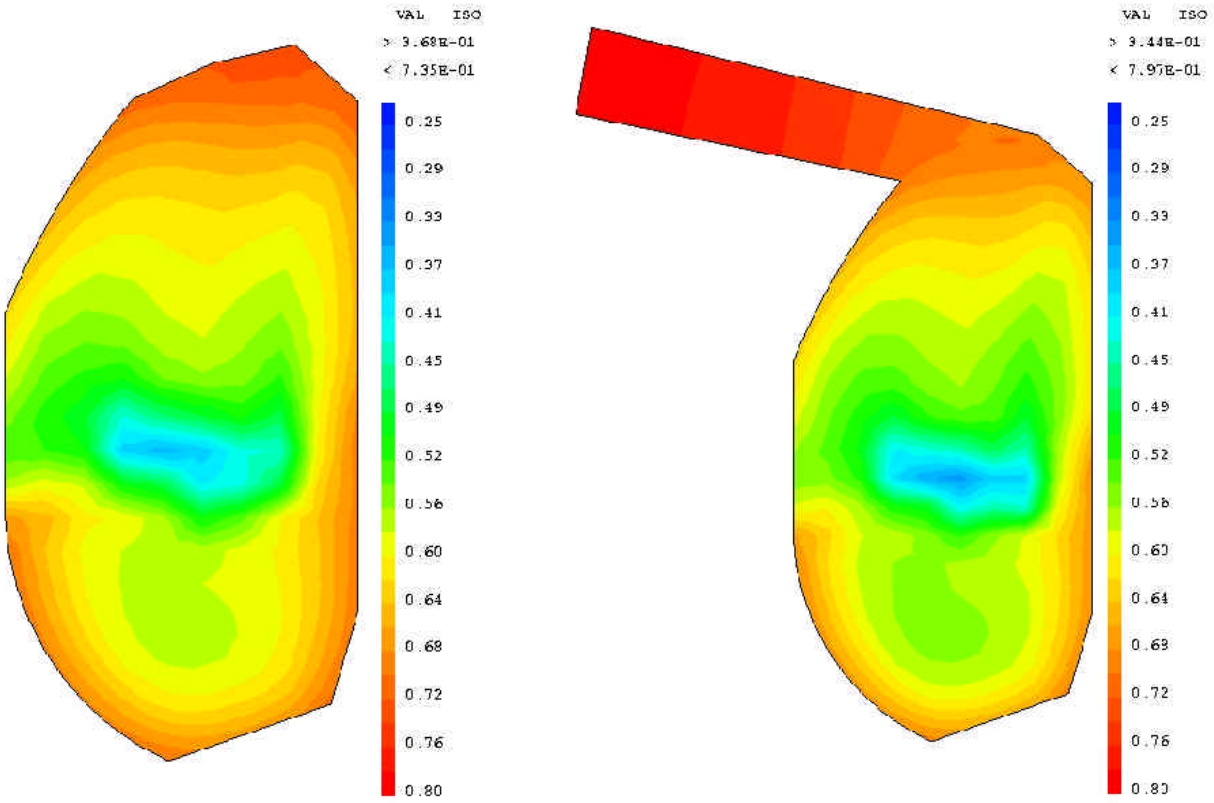

Figure 2 : Hydrogen volume fraction before the air ingress

CONCLUSIONS

A calculation of hydrogen distribution within the ITER vacuum vessel in case of in-vessel LOCA has been done, which allows to draw first conclusions on the general trends. It must be kept in mind that the results are sensitive to the initial conditions (characteristics of the break, gas concentrations, …).

REPORTS AND PUBLICATIONS

N. Coulon, Simulation of H2 detonation in the ITER-FEAT vessel with the CAST3M ITER code, CEA report SFME/LTMF/RT/02-005/A.

A. Bleyer, F. Dabbene, Simulation of H2 distribution in the ITER-FEAT vessel with the CAST3M-ITER code, CEA report SFME/LTMF/RT/02-032/A.

TASK LEADER

Pierre SARDAIN

DER/SERI/LFEA
CEA Cadarache
13108 Saint Paul Lez Durance Cedex

Tél. : 33 4 42 25 37 59
Fax : 33 4 42 25 36 35

E-mail : pierre.sardain@cea.fr

TW1-TSS-SERF2

Task Title: TRITIUM RELEASES AND LONG TERM IMPACTS

INTRODUCTION

The objective of this study was to perform a in-deep analysis of ^{3}H releases in the environment and their long term impacts, as it was initiated in the SERF-2 study [1], both for routine and accidental releases. It paid a special attention to the potential contamination of agricultural foodstuffs in accidental situation and their marketing restrictions with regard to national regulations about tritium.

In a first phase, the task has consisted in reviewing both the recent developments on transfer modelling of ^{3}H in the environment, collecting the available measurements of ^{3}H in the environment and foodstuffs for different countries and finally synthesizing the existing regulations in different countries with regard to ^{3}H contamination in foodstuffs. In a second phase, calculations of radiological impacts of ^{3}H releases in the environment were performed with the computer codes UFOTRI [2] and NORMTRI [3]. Time dependent activity concentration in food and doses to the public in a 100 km-radius area around a fusion installation were discussed and compared with measurements into the environment in the case of routine releases and with the regulatory limits in foodstuffs in case of accidental releases.

2002 ACTIVITIES

Guidelines and regulatory limits in countries

Regulatory limits for tritium in foodstuffs in different countries or guidelines provided by different international organisations were collected for normal and accidental situations. Corresponding values are presented in table 1 and table 2.

In normal situation, values vary from 100 Bq/L in many European countries to 10,000 Bq/L or kg in Switzerland.

In accidental situation, it must be noticed that no well-defined intervention criteria has been found in the EC regulations, but only guidance values under discussion.

Environmental measurements

Measurements of ^{3}H in the environment are available close to nuclear facilities.

In France, some data have been collected (concerning mainly ^{3}H activity concentration in water).

Table 1 : Values concerning tritium in water (Bq/L) or food (Bq/kg) in different countries and organisations, in normal situation

Country or organism	Value	Status*
World Health Organisation	0.1 mSv/year (all radionuclides) 7,800 Bq/L (if only tritium)	Guidelines value Reference value (calculated)
The European Council	100 Bq/L	Limit value (parametric)
France	100 Bq/L	Limit value (parametric)
Germany	100 Bq/L	Limit value (parametric)
United Kingdom	100 Bq/L	Limit value (parametric)
Sweden	100 Bq/L	Limit value (parametric)
Belgium	100 Bq/L	Limit value (parametric)
United States - US-EPA - OEHHA - DHS (California)	 0 Bq/L - 0.04 mSv/year - 740 Bq/L	Guidelines value (MCLG**) Limit value (MCL) Guidelines value (PHG) Limit value
Canada	7000 Bq/L	Limit value
Switzerland	1,000 Bq/L or kg 10,000 Bq/kg or L for foodstuffs and drinking water, 100,000 Bq/kg for food of less important, 3,000 Bq/kg for babies food	Tolerance value Limit value

Table 2 : Values concerning tritium in water (Bq/L) or food (Bq/kg) in different countries and organisations, in case of nuclear accidental situation

Organisation	Criteria for Tritium
WHO	Calculated for tritium: 400,000 to 2,400,000 Bq/L or kg depending on the food (if only tritium)
Codex	Calculated value (CEPN): about 1,000,000 Bq/L or kg (if only tritium)
IAEA	Calculated value (CEPN): about 1,000,000 Bq/kg for foods for general consumption and about 100,000 Bq/kg or L for milk, infant foods and drinking water (if only tritium)
ICRP	Calculated value (CEPN): between 1,000,000 and 10,000,000 Bq/kg (if only tritium)
EC	From 4,000 Bq/kg or L for baby foods to 125,000 Bq/kg or L for minor food (milk products: 10,000 Bq/L; other food: 12,500 Bq/kg)
USFDA	Calculated value (CEPN) as for others nuclides: 300,000 Bq/kg for organically bound tritium and 725,000 Bq/kg for free tritium (if only tritium)
Canada	30 000 Bq/kg for fresh liquid milk 100 000 Bq/kg for commercial foods and beverages 100 000 Bq/L for public drinking water (if only tritium)
France	As for EC
Belgium	As for EC
Germany	As for EC
UK	As for EC
Switzerland	For tritium (concerning natural radionuclides): - Tolerance value of 1000 Bq/kg or L - Limit value: 10 000 Bq/kg or L for foodstuffs and drinking water, 100 000 Bq/kg for food of less importance, 3 000 Bq/kg for babies food Applied independently between radionuclides groups; additive within single group of radionuclides

IMPACTS OF TRITIUM RELEASED IN THE ENVIRONMENT

Radiological impacts and foodstuffs contaminations associated with ^{3}H release from a fusion power plant under both normal and accidental situations were calculated. The influence of several parameters has been tested by considering several sets of release conditions. This included 3 different release heights and 5 different weather conditions under accidental release conditions.

POTENTIAL FOOD BANNING IN CASE OF ACCIDENTAL SITUATION

The aim was to investigate the possible need for food banning in accidental situation. For that purpose, the ^{3}H release was set to 50 g of HTO, value considered in SERF-2 study. For each category of food products, e.g. cow milk, green vegetables, root vegetables (potatoes), grain (wheat) and cow meat, the total number of days for which the tritium contents exceed the regulatory limits were calculated as well as the corresponding surface area. These results were then combined with the agricultural production data in order to calculate the total amount of food products to be lost. As far as at present there is no well defined tritium concentration limit values for foodstuffs in European countries regulations regarding to emergency situations, two sets of limit values were considered (table 3). Set 1 refers to proposed guidance values, currently under discussion at the European level. Set 2 is based on derived values from IAEA methodology.

These two sets can be interpreted as lower and upper bounds of tritium concentration limits in foodstuffs.

Table 3 : Concentration limit values for tritium in food products in emergency situations

Limits Set 1	- 10 000 Bq/L for milk - 12 500 Bq/kg for meat, grain, green and root vegetables
Limits Set 2	- 220 000 Bq/L for milk - 280 000 Bq/kg for meat - 430 000 Bq/kg for green and root vegetables - 370 000 Bq/kg for grain

With Set 1 limit values, up to 30 000 km^2 can exceed the maximum permissible level (HTO) for at least one day. Leafy vegetables were identified as the food being responsible for the largest area. It has to be noted that mainly HTO in the crop causes the high concentrations in the short tem and not the OBT fraction.

Therefore, the area above the level becomes much smaller after one week. In case of the release scenario night and a 10 m release height, the initial 30 000 km^2 drop to about 9 000 km^2 and now milk is the decisive food. After one month, the area affected diminishes to about 300 km^2 with milk or cereals still above the permissible levels.

The picture changes completely when higher permissible activity levels in food are applied (Set 2). The largest affected area only reaches 1 000 km^2.

ACTIVITY CONCENTRATIONS IN THE ENVIRONMENT FOR ROUTINE RELEASES

Routine releases of 1g of HTO were considered for 3 different release heights with the meteorological conditions of the year 1991 for the Cadarache site. Activity concentration in food strongly depends on the food type. Highest tritium concentrations close to the fence at 1 km distance were obtained for leafy vegetables with values close to about 3 500 Bq/kg. Even for milk, the concentration easily exceeds 1 000 Bq/L. Both activity concentrations were observed for the near ground level release. A more realistic scenario with elevated releases reduces both values to about 800 Bq/kg and 300 Bq/L for leafy vegetables and milk, respectively. Activity concentrations for other foods are in the order of 100 to 200 Bq/kg, a range that is not too unusual also for current installations. However, the release of 1 g of HTO over one year is not a realistic target for ITER or a fusion reactor, but was used to have a screening value.

Nevertheless, regarding values measured in the environment, ^3H activity concentration in milk near nuclear facilities never exceed 100 Bq/L and 300 Bq/kg in vegetables and the calculated values with a lower quantity of ^3H released would be in the same range. It is important to outline that ^3H contamination linked to routine release from a fusion power plant are not insignificant.

CONCLUSION

This study has resulted, on the one hand, in a detailed review of tritium regulatory limits in major foodstuffs for different countries or international organisations. On the other hand, it has produced an in-deep evaluation of the radiological impacts of tritium released into the environment, by considering recent dispersion models as well as a wide panel of release conditions. A sensitivity analysis of the results with the major model parameters studied was performed. Tritium activity concentrations in foodstuffs in case of a deterministic accident scenario as the one considered in SERF-2 have been calculated and compared with two sets of “present” regulatory limits, in order to determine the areas around the site which could be temporarily concerned by food banning. Results from this study served as an direct input to SERF-3 study on the evaluation of external costs of a fusion accident (related Task TW1-TRE-ECFA-D2).

REFERENCES

[1] SCHNEIDER T., LEPICARD S., Evaluation of radiological and economic consequences associated with an accident of a fusion power plant, SERF2 Subtask 1.1.8, CEPN-NTE/00/08, 2000.

[2] RASKOB, W.,UFOTRI: Description of the New Version of the Tritium Model UFOTRI 4.0, including user guide. Report KfK-5194, Kernforschungszentrum Karlsruhe, 1993.

[3] RASKOB, W., Description of the Tritium Model NORMTRI for Releases under Normal Operation Conditions. Report KfK-5364, Kernforschungszentrum Karlsruhe, 1994.

REPORTS AND PUBLICATIONS

LEPICARD S., RASKOB W., VAILLANT L., BENHAMOU C., SCHNEIDER T., Impacts associated with a tritium release from a fusion power plant, CEPN-NTE/02/38, 2002.

TASK LEADER

Thierry SCHNEIDER

CEPN
Route du Panorama
Boîte Postale 48
92263 Fontenay aux Roses Cedex

Tél. : 33 1 58 35 76 59
Fax : 33 1 40 84 90 34

E-mail : schneider@cepn.asso.fr

TW1-TSW-002

Task Title: WASTE AND DECOMMISSIONING STRATEGY

INTRODUCTION

This study is devoted to the management of tritiated materials. A process is currently used in CEA Valduc to detritiate steels. It is based on a melting of steel under vacuum. This allows a volume reduction of the wastes and a drop of tritium activity from 1000 Ci/t to 10 Ci/t (average activities). Since the detritiation factor needs to be enhanced, possible improvements to this existing process were studied based on steel industry for pollution reduction concerning hydrogen, carbon and nitrogen. An argon bubbling is performed to favour surface reaction. A modelling, developped for hydrogen was adapted to tritium.

The second point of this study concerns a limitation of tritium release from ingot after melting. The addition of substances or the modification of the micro structure which could stabilise hydrogen isotopes in the material are studied.

2002 ACTIVITIES

IMPROVEMENT OF THE DETRITIATION PROCESS

An adaptation of the melting facility has been proposed. In a first step this adaptation concerns argon bubbling. The following step could consist in argon and hydrogen bubbling to favor isotopic exchange.

This facility is to be waiting for the French Safety requirements. The 2002 activities were dedicated to the adaptation of the facility to take into account these requirements. Thus it was not possible to perform the work for fusion activities.

POSSIBILITIES TO DECREASE TRITIUM RELEASE

Preliminary studies have been performed on samples coming from an ingot produced in CEA/Valduc (before facility expectation) and which was characterized by auto radiography.

Material characterization

A material characterization has been performed by optical microscopy and Scanning Electron Microscopy (SEM) after polishing and acid etching. These observations show the presence of a complex microstructure which is characteristic of a raw state. A significant fraction of δ ferrite is also present.

Different precipitates can also be found and characterized by the X analysis of the SEM: manganese sulfide, chrome and titanium carbides (very small sizes), phase with high concentration in niobium and other precipitates which, like δ ferrite, are enriched with chromium and molybdenum.

The tritium contents have also been characterized. The measurement has been done by liquid scintillation after dissolving about 1 g of material in acid solution (HCl 45 %, HNO_3 5 % and H_2O 50 %vol). This acid solution (containing the dissolved metal) is then diluted to increase the pH, and tone down the solution. About 1 cm^3 of this solution is added to 15 cm^3 of scintillation cocktail for analysis. This has been done for 2 samples (see table 1) and we may observe a dispersion of the mean activity (tritium).

Table 1 : Tritium activity measured by liquid scintillation

Sample	Mass (g)	Activity (kBq/g)
D1	0.780	14.4
D2	1.028	5.7

Moreover, these values are 5 to 10 times lower than the activities previously measured.

Even if radioactive decay and tritium out gassing can partly justify this difference, these results lead to an improvement in the measurement procedure by addition of a tritium measurement on the gaseous effluents.

Desorption measurements

The technique consists in the realization of β counting by liquid scintillation to determine the residual tritium which desorb from a bulk metallic sample, with a known dimensions directly immersed in the scintillation liquid. The measured values were corrected with respect to the quenching effect related to the presence of a solid in the scintillation liquid. Two values can be obtained: surface activity and desorption kinetics of the residual tritium (see figure 1).

The surface activity (expressed in $Bq.cm^{-2}$) is obtained directly after immersion of the sample. It represents the tritium concentration in a superficial layer of the metal, the thickness being linked to the escape distance of the electrons typical of the tritium β radiation.

Concerning residual tritium desorption, the counting allows the determination of the extracted tritium as a function of time. Based on activity increase as a function of immersion time, the mean value of the kinetic desorption can be obtained (expressed in $Bq.cm^{-2}.s^{-1}$).

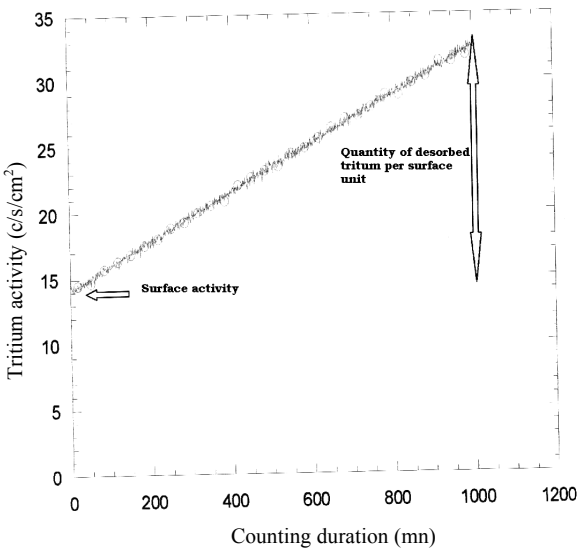

Figure 1 : Tritium activity as a function of counting duration

The influence of thermal treatment on desorption was studied:

- measurement of the tritium desorption kinetic after polishing and during 1 hour,
- thermal treatment, at 1050°C during 1 hour,
- measurement of the tritium desorption kinetic during 1 hour.

The thermal treatment leads to the formation of a thick oxide film at the surface of the sample. This layer was removed by polishing and then the tritium desorption kinetics measured once again. The results are given in table 2.

Table 2 : Influence of heating treatment on desorption medium flux after 1 hour at 20°C

Sample 2A	Desorbed quantity after 1 hour at 20°C (dpm)	Medium flux ($Bq.cm^{-2}.s^{-1}$)
Before heating treatment	300	$5.0\ 10^{-4}$
After heating treatment and before second polishing	2	$3.0\ 10^{-6}$
After heating treatment and after second polishing	3	$5.0\ 10^{-6}$

Table 2 shows that:

- The heating treatment at 1050°C during 1 hour leads to an important decrease of the surface activity (desorption kinetics about 100 lower after the treatment).

- The presence of an oxide layer (due to the thermal treatment) leads to an increase of the surface activity. This indicates that in comparison with the bulk material, the oxide layer is enriched in tritium. This was also observed in [1].

- For the low values of residual tritium (after heating treatment), there is no significant barrier effect due to the oxide film since there is no significant difference between the desorbed quantities.

CONCLUSIONS

As the CEA Valduc melting facility is waiting for safety authorization, only the second part of the study was performed in 2002. The micro structure study of the previous ingot confirms the presence of a complex micro structure in which different phases can favor the interaction with the tritium (in particular trapping reactions).

The residual tritium values are 5 to 10 times lower than the activity previously measured. Even if radioactive decay and tritium out gassing can justify a part of this difference, these results leads to improve the measurement procedure by adding a tritium measurement on the gaseous effluents. The conditions of sample preparation and counting were optimized to improve the reproducibility of the liquid scintillation results.

And the preliminary study on the impact of thermal treatment shows that these conditions (1050°C, during 1 hour) lead to an important decrease of the residual tritium and its desorption kinetic.

REFERENCES

[1] P. Lacombe, M. Aucouturier, J. Chêne, 'hydrogen trapping and hydrogen embrittlement" in hydrogen embrittlement and stress corrosion cracking, publication ASM, ed R. Gibala and RF Hehemann, (1984), pp 79-102.

REPORT

J. Chêne, A.M. Brass, M. Hamdi, "Tritiated waste management", report from the Laboratoire de physico-chimie de l'état solide, CNRS, UMR 8648, ICCMO, Université Paris Sud, dec 2002, to be translated.

TASK LEADER

Sandrine ROSANVALLON

DEN/DER/STR/LCEP
CEA Cadarache
13108 Saint Paul Lez Durance Cedex

Tél. : 33 4 42 25 64 19
Fax : 33 4 42 25 72 87

E-mail : sandrine.rosanvallon@cea.fr

JW0-FT-2.5

Task Title: TRITIUM PROCESSES AND WASTE MANAGEMENT Dedicated procedures for the detritiation of selected materials

INTRODUCTION

Since the Preliminary Tritium Experiment (PTE) in 1991, tritium has been used in the Joint European Torus (JET) in Culham. Due to its high diffusivity and different trapping phenomena, tritium is present in the first wall materials.

From waste management point of view, it is necessary to reduce tritium inventory before disposal since countries regulation already limit tritium contents and releases. Two different strategies can be adopted for tritiated waste management. The first one consists in waiting for radioactive decay. The second one consists in the application of detritiation processes.

For many years, studies have been performed to determine the different processes that could be used for tritium removal.

The aim of this task was, first, to list the different processes which can be used for carbon materials and stainless steels. Then the most promising ones were selected. Finally, further studies were launched to validate this selection.

2002 ACTIVITIES

Detritiation process on stainless steel:

After a bibliography study, it has been noticed that steel detritiation occurs from 573 K and above [1]. Tritium diffusion is negligible when tritium is combined as HTO and HTO is generated at such a high temperature[2].

During this period, the LCEP laboratory has developed a comprehensive procedure to extract tritium from steel, this has been performed by thermal outgassing under air atmosphere. An inter-laboratory comparison with a CEA laboratory located at Saclay has been done to meet the requirement of good laboratory practice. To check the good detritiation level, another procedure is under application : a full dissolution of steel sample with hydrochloric acid solution. Steel samples were originated from a French fast breeder reactor plant to be decommissioned.

Graphite samples :

Concerning graphite, our laboratory did not get actual sample from JET, however commercial graphite has been fully mineralised to permit a potential full tritium recovery.

TECHNICAL RESULTS

Analyses were performed on rather small quantities of steel, knowing that our laboratory is presently limited in terms of radioactivity levels and safety regulation.

Weighed sample (about 700g) was dropped in an hastelloy container heated under air atmosphere, the volume of this container was design to be able to receive samples of 10 cm diameter and 5 cm high. Detritiation of samples were performed in a furnace at 1273 K. Then to check the total release of tritium, one more step has been done at 1323 K.

Downstream the container a MARC 7000 system has been set to recover and convert tritium to tritiated water (photography); gas flow-rate was set to 35 L/h. Detritiation was done under to different atmospheres to check the behaviour of tritium species, and sampling was also performed at intermediate temperatures.

Table 1 : Results of detritiation of stainless steels under 2 different atmospheres (Hytec = 5 % of hydrogen in argon matrix)

	Air				Hytec			
	HTO Bq	HT Bq	total ^{3}H Bq	total ^{3}H Bq/g	HTO Bq	HT Bq	total ^{3}H Bq	total ^{3}H Bq/g
673 K 3 hours	2220	14	2234	30	870	1185	2055	38
1273 K ½hour	605	6	611	8	50	220	270	5
1323 K 1 hour	17.5	-	17,5	0,25	11	9	20	0,4
total ^{3}H in sample	2842	20	2862	**38,3**	931	1414	2345	**43,4**

Results are within the same range with associated uncertainty of about 15 % for the whole procedure.

Photography : furnace and MARC 7000 for tritium recovery

An inter-comparison exercise has been set up with another CEA laboratory located at SACLAY. Satisfactory results in agreement are listed in the table here under, knowing that the other laboratory used the melting technique with an inductive oven (table 2):

Table 2

		Sample 1	Sample 2
LCEP		Bq/g	Bq/g
	Air	38,3 (08/04/02)	11 (16/10/02)
	Hytec	43,4 (26/09/02)	19,8 (22/10/02)
Saclay			
	melting	37,4 (07/10/02)	20,3 (03/10/02)

To know the tritium behaviour and its possible distribution within the steel matrix our laboratory has measured the tritium content in thin layers located at the surface of sample. This work has been performed on a 1380 g of steel sample; sizes of this sample were : diameter = 10 cm ; total thickness = 2.25 cm. This mineralization of thin layers was performed with hydrochloric acid, tritiated species were isolated. For instance, tritiated solutions were distilled to be counted by liquid scintillation.

Hydrogen (associated with tritium) release was converted to water through a catalytic oxidizer, to get the tritiated water, then this water was counted by liquid scintillation.

The results are expressed as percentage of tritium in these layers compared to the total tritium of the sample measured by thermal detritiation (table 3).

A large amount of tritium is distributed within the first thin (less than 10 µm) layer; a depth lower than 70 µm contains about 21 % of total tritium, this means 5.71 g of steel (i.e. 0.4 % of metal weight). Consequently this means that tritium concentration is depleted in bulk.

Graphite :

No actual samples have been tested, however the laboratory developed a methodology to fully oxidize graphite.

This is a wet ashing procedure which enables the elimination of carbon as carbon oxide species, tritium should be also eliminated and distributed in different phases, depending upon the original form linked to graphite.

This techniques, different from dry ashing, will allow the measurement of both chemical and radio-chemical impurities of graphite.

CONCLUSION

During this period, the LCEP laboratory has developed a comprehensive procedure to extract tritium from steel, this has been performed by thermal outgassing under air atmosphere. An inter-laboratory comparison with a CEA laboratory has been done to meet the requirement of good laboratory practice.

To check the good detritiation level, another procedure is under application : a full dissolution of steel sample with hydrochloric acid solution. Currently the laboratory develops procedure to extract tritium in different matrices such as inconel, plastics and in a near future: concrete.

Concerning graphite, our laboratory did not get actual sample from JET, however commercial graphite has been fully mineralised to permit a potential full tritium recovery.

Table 3

	Mass of dissolved Steel in g	Metal thickness µm	% tritium liquid phase	% tritium gas phase	% of total tritium
First layer	0.43	6.5	10.2	0.1	10.3
Second layer	1.52	22.5	8.1	0.1	8.2
Third layer	4.76	70.4	2.4	0.1	2.5

REFERENCES

[1] A. PEREVEZENTSEV - Contamination of stainless steel type 316 by tritium - UKAEA Culham science centre - Abingdon, OX14 3DB, UK.

[2] J.L. COUROUAU - Précalcul de la migration du tritium à travers le confinement de CASCAD 2 pour l'entreposage du carbure de bore et du béryllium irradié - DER/STR/LCEP 00/060.

TASK LEADER

Christian POLETIKO

DER/STR/LCEP
CEA Cadarache
13108 Saint Paul Lez Durance Cedex

Tél. : 33 4 42 25 64 93
Fax : 33 4 42 25 72 87

E-mail : christian.poletiko@cea.fr

UT-S&E-LASER/DEC

Task Title: LASER DECONTAMINATION: TRITIUM REMOVAL

INTRODUCTION

In the case of D-T fusion reactors, tritium is trapped in a co-deposited layer which results from the sputtering of the surface of plasma facing components (C, Be, stainless steel) by plasma during reactor operation. Re-deposition of the sputtered particles together with hydrogen, deuterium and tritium takes place on colder areas inside the reactor.

The tritium inventory trapped in this layer could threatened ITER operation. For this purpose we are developing both an experimental and a simulation program in order to study the efficiency of a possible laser-based detritiation process.

A first part of our work has consisted to implement a laser bench to work as well with infra-red (1064 nm), visible (532 nm) and ultra-violet (355 nm) wavelengths and allowing to well characterize the laser fluence on the sample.

Then, first ablation experiments have been performed. A thermal modelisation tool has also been developed and feasibility tests with a diagnostics allowing to follow in real time the co-deposited layer removal have been realised.

2002 ACTIVITIES

EXPERIMENTAL SET-UP AND BEAM METROLOGY

Our first aim is to measure ablation thresholds and rates. For this purpose it is therefore necessary to well characterize the laser beam used to perform ablation.

Two main parameters are highly relevant and have been measured : the total energy of the beam incident on the sample surface and the spatial energy distribution at the place of laser-matter interaction.

For this purpose, the experimental set-up described below (see figure 1) has been implemented. The beam of a Brilliant laser manufactured by QUANTEL (5 ns pulse duration, 20 Hz repetition rate) reflected by two mirrors (M1 and M2), is focused by a lens (L1) and scanned by a motorised mirror (M5) on the sample.

The beam is characterized , by two leaks (transmissions of the mirrors), the first one after the M2 mirror and the second one after the M5 mirror which are analysed by a joule-meter (to measure the laser beam energy) and a CCD camera (to record the spatial energy distribution of the laser beam, see figure 2) respectively.

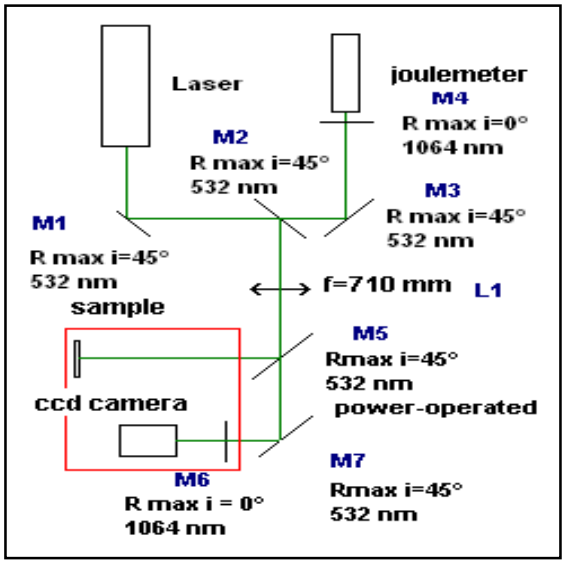

Figure 1 : Experimental set-up

The experiments have consisted to measure beam parameters for three wavelengths (1064 nm, 532 nm and 355 nm). Figure 1 shows the set-up optimised for 532 nm wavelength. To perform measurements for other wavelengths, it is necessary to use optical components adapted to the wavelength of interest.

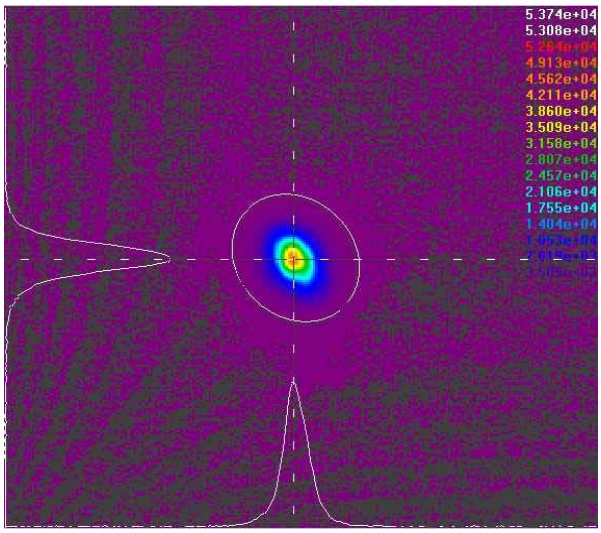

Figure 2 : Laser beam energy distribution on the sample

SAMPLES

The graphite (isotropic graphite CL 5890 PL) samples that we tested are from the H-D fusion reactor TORE-SUPRA of CEA in Cadarache. They are parts of tiles from the belt limiter that were exposed to 25000 disharges with ion-temperatures of about 1 keV. The exposition was of the order of 30 seconds.

The co-deposition layer has been analysed by scanning electron microscopy (see figure 3) associated with EDS analysis (see figure 4). The structure of the co-deposited layer looks like aggregates. The EDS analysis show that impureties like Fe and Cr are present in this layer, coming from sputtered structural components made in stainless steel. Such impureties have already been described and are specific of the co-deposition phenomenon.

Unfortunately, at the present time the thickness of the co-deposited layer has not been successfully measured and complementary analysis by SEM are under progress.

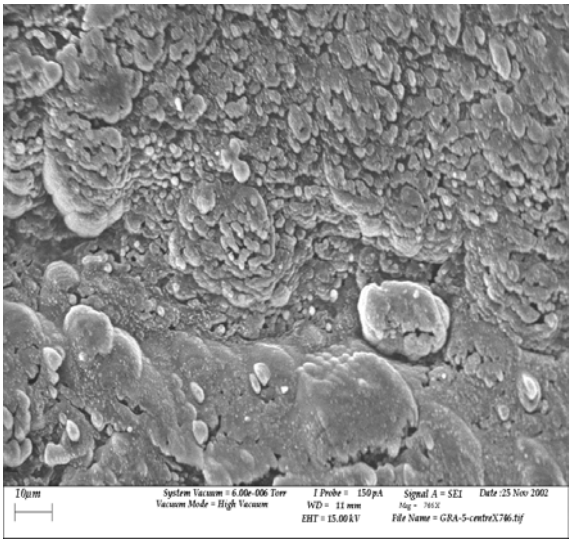

Figure 3 : Co-deposited layer by SEM

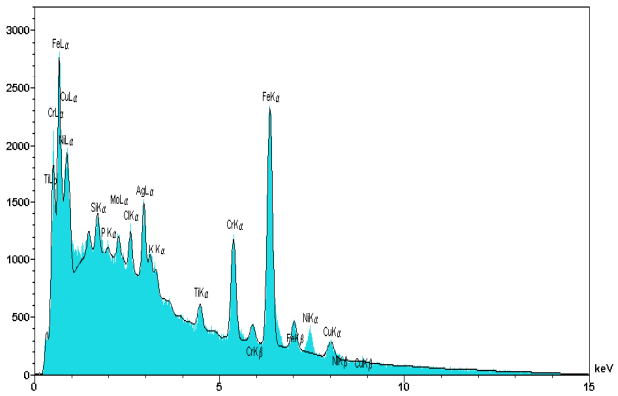

Figure 4 : Co-deposited layer by EDS

EXPERIMENTAL RESULTS

In both cases, samples have been submitted to 500 shots with variable fluences. The ablated volumes (craters) have been measured by means of a profilometer. The following curves (see figures 5 and 6) present results of ablation. Such curves allow to estimate both the ablation threshold (AT) and the volume ablated per shot.

Two regimes of ablation can be observed :

- a quite linear variation of ablated volume versus fluence up to 9 J.cm^{-2},
- a very low rise versus increasing fluence since 13 J.cm^{2}.

In order to estimate the ablation threshold of graphite, points corresponding to the first regime have been plotted and a linear regression has been applied. Taking into account the linear equation obtained, the deduced ablation threshold of graphite is about 1 J.cm^{-2}.

Furthermore, the two regimes identified above can be explained as follow : In the first regime, the interaction occurs between the laser and the surface while in the second case, the plasma is more hot and its density higher, leading to an absorption of laser energy by the plasma. Then an interaction takes place between the plasma and the surface. This can be demonstrated when looking at the sizes of craters observed in the second case. Indeed, the characteristics diameters at the surface of the crater are much higher (up to 800 µm) than those of the laser spot (about 300 µm). It appears clearely that for a detritiation process, in order to optimize the efficiency in term of velocity, the first regime has to be chosen.

As mentionned above, the thickness of the co-deposited layer is unknown. Nevertheless, when comparing respective ablated volumes at 2.7 J.cm^{-2} of the graphite sample with co-deposition (see figure 6) and the back side of another graphite sample (see figure. 5), the volume removed in the first case seems to be 3 times higher. This first result on co-deposited layer ablation rate, which seems to be higher than graphite one, has to be confirmed by additionnal test on better characterized sample in term of co-deposited layer thickness.

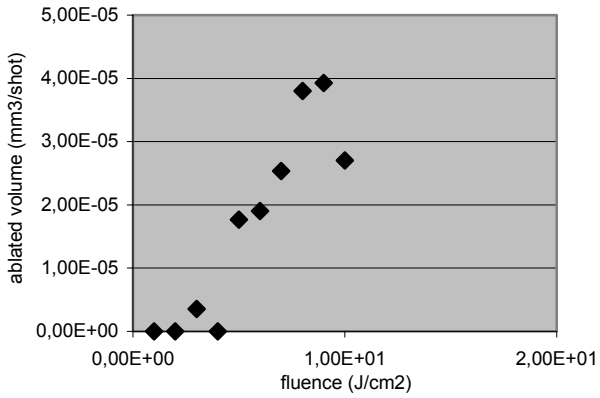

Figure 5 : Ablation measurements on graphite

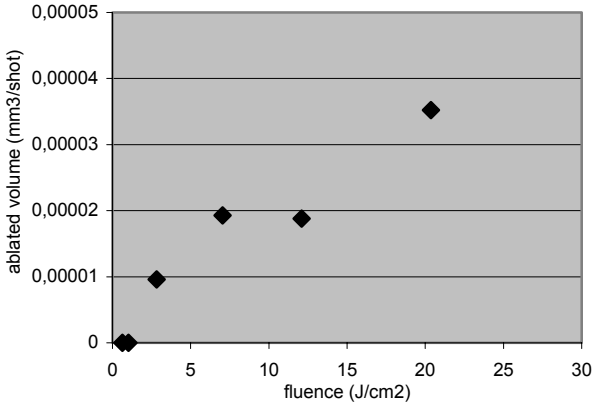

Figure 6 : Ablation measurements on graphite + co-deposited layer

THERMAL MODEL

In order to simplify optimisation and to determine efficient operation parameter ranges of a future laser-based process we develop in parallel to experiments a laser-matter interaction modelisation. Furthermore, facilities available at DPC/SPAL don't allow to perform experiments on beryllium (Be). As a first stage, a simple one dimensional tool has been developed allowing to calculate the energy deposition in the material and its thermal behaviour, during and after energy deposition taking into account thermal conductivity.

The modelisation is based on a numerical resolution of the heat equation. Calculations have been performed (see figure 7) in case of graphite taking into account incident laser (532 nm) fluences of 0,7 J/cm^2 and 1 J/cm^2 respectively. Taking into account the boiling point of graphite (4623°K), it can be deduced from numerical results that its ablation threshold is comprised between 0,7 J.cm^{-2} and 1 J.cm^{-2}. Such a result is in good agreement with the experimental estimation (see "Experimental results"). Similar calculations, performed for Be, indicate that its ablation threshold is comprised between 0.5 J.cm^{-2} and 0.75 J.cm^{-2}.

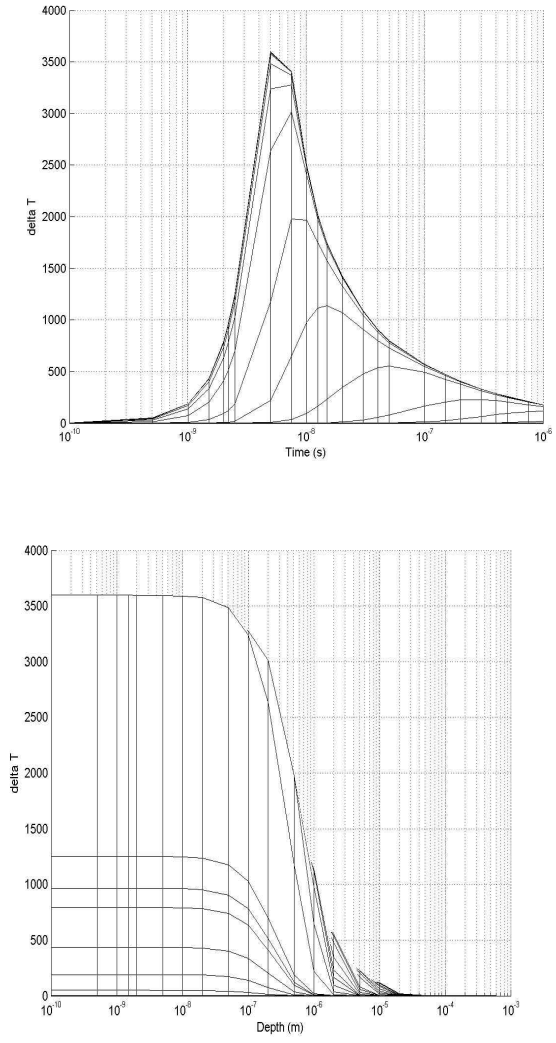

Figure 7 : Temperature depth and time distributions for graphite (0.7 J/cm^2)

FEASABILITY TESTS PERFORMED WITH AN OPTICAL EMISSION SPECTROSCOPY DIAGNOSTIC

Post-test analysis are time and cost consumers. For this reason we have decided to implement a real time diagnostic in order to reduce the number of surface analysis (SEM, Luminescent Discharge Spectroscopy…) to perform before and after laser-matter interaction tests.

The Optical Emission Spectroscopy has been quickly identified as a very promising candidate for three main reasons:

- It allows by recording lines emitted from the laser induced plasma to characterize the surface in term of chemical element composition. It is therefore possible to follow the decontamination by recording in real time specific lines of the contaminated layer or of the substrate;

- it is a very sensitive technique (low detection threshold < ppm);

- it is convenient to implement (no necessary vacuum, signal collected by optical fibres allowing to let expensive devices outside the contaminated zone).

The first experiments performed have consisted of identify the 247.856 nm line of carbon.

A single laser shot has been delivered on a graphite sample (without co-deposition) and the spectrum presented on the figure 8 has been obtained.

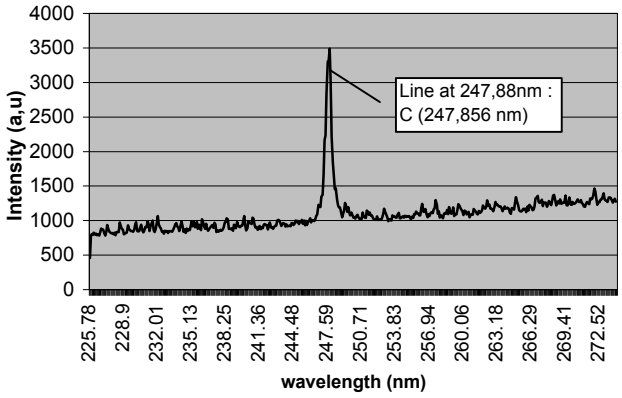

Figure 8 : Graphite spectrum

This experimental result is in a very good agreement with the expected value. The same experiment has been repeated on the sample with a co-deposited layer in order to record the co-deposited layer spectrum (see figure 9).

This one reveals the presence of Fe and Cr which have already been identified by the EDS analysis (see figure 4).

Nine additional shots have then been done on the same location than the first shot and the plasma emission has been recorded during the plasma created by the last shot.

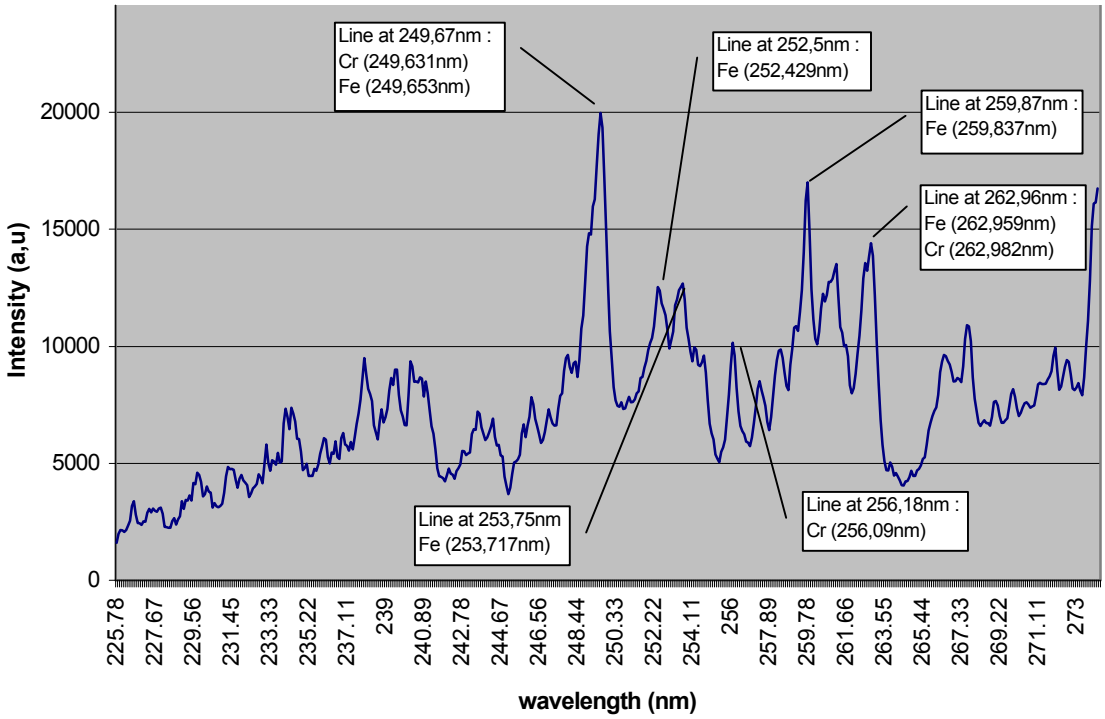

Figure. 9 : Comparison of spectra

The corresponding spectrum is represented in yellow on the figure 10 and compared to specific spectra of co-deposited-layer in violet and graphite in blue. It appears that the specific spectrum of the co-deposited layer has nearly disappeared except a residual line specific of Fe or Cr (the resolution of the device doesn't allow to discriminate).

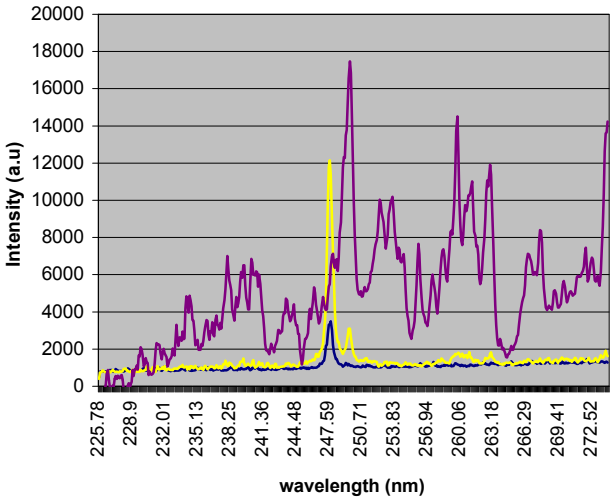

Figure 10 : Co-deposited layer spectrum

A post-analysis EDS performed on a graphite sample with co-deposited layer irradiated by laser in similar conditions is shown on the figure 11.

When comparing the recorded spectrum with another one realised on the same sample (see figure 4) before laser treatment, a decrease of metallic line intensities can be observed, and confirms qualitatively the observations obtained with optical emission spectroscopy. The presence of Fe or Cr is probably due to a diffusion of this impurity deep in the bulk of graphite. The depth of diffusion must be estimated in further studies.

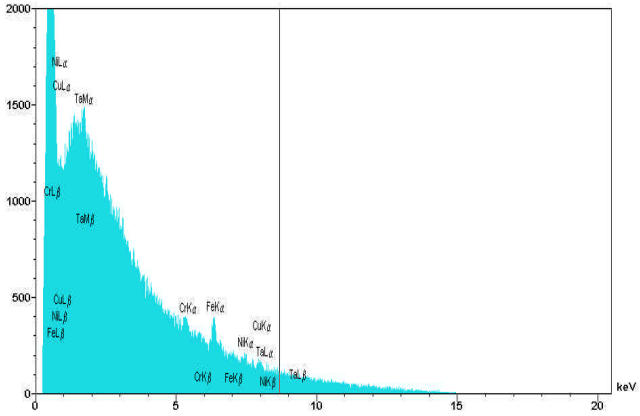

Figure 11 : EDS analysis after laser treatment

CONCLUSION

In this first part of the research work, a laser bench has been implemented which allow to perform well controlled ablation experiments with ultra-violet, visible and infra-red wavelengths.

Furthermore a protocol to estimate ablation thresholds and rates for variable materials is now available. First ablation measurements have been obtained at 532 nm for TORE-SUPRA samples. It seems that the co-deposited layer is removed at this wavelength more easily than graphite, but this has to be confirmed.

A thermal model has been developed and gives quite good results in term of ablation threshold prediction.

Finally we have performed feasibility tests with an Optical Emission Spectroscopy device.

We have demonstrated that such a method allows to discriminate the graphite and the co-deposited layer thanks to specific lines of Fe and Cr, elements present in the co-deposited layer. This diagnostic will permit both to decrease the number of analytical tests needed to optimise laser detritiation and to follow in real time co-deposited layer removal (in order to avoid or limit tile deconditionning).

REPORTS AND PUBLICATIONS

Bibliography study on co-deposited layer and laser detritiation processes.
Le Guern, Weulersse
DEN/DPC/SPA/LLA/2003.06.

Laser decontamination tritium removal
Le Guern et al
DEN/DPC/SPA/LLA/2003.02.

TASK LEADER

F. LE GUERN

DEN/DPC/SPAL
CEA Saclay
91191 Gif-sur-Yvette Cedex

Tél. : 33 1 69 08 79 78
Fax : 33 1 69 08 86 91

E-mail : leguern@carnac.cea.fr

UT-S&E-Mitig

Task Title: EVALUATION AND MITIGATION OF THE RISK CONNECTED WITH AIR OR WATER INGRESS

INTRODUCTION

In case of water ingress in the torus, for instance due to a breach of the first wall (beryllium) between torus itself and cooling system, the beryllium oxidation leads to hydrogen production (Be + H_2O ➡ BeO + H_2), with the explosion risk associated. It is therefore necessary to define a strategy in order to mitigate this risk.

An hydrogen elimination process, based on the reduction of a metallic oxide mixture has been studied, which allows to convert gaseous hydrogen into water (H_2 + MnO_2 ➡ MnO + H2O), even if oxygen concentration remains very low. The present study is aimed to the design of an apparatus dedicated to ITER.

2002 ACTIVITIES

This was the final year for this study. This program was aimed to the development of a mitigation system for hydrogen risk, including experimental program and kinetics parameters determination, to develop a computer tool (MITHRY) and first design for a mitigation system, based on ITER accident scenarii.

This report summarizes the main results achieved during this study. Basically, the process is based on the reduction of metallic oxide (MnO_2) by hydrogen, to produce water and manganese sub-oxides. A small part of silver oxide (Ag_2O) is added to the manganese dioxide, in order to promote the reaction, especially at low temperature (ambient to 150°C).

The raw product is a mixture of manganese dioxide and silver oxide powders with thin granulometry, below 100 µm. It was thus necessary to develop a shaping method, so that it can be easily handled. Two ways were investigated:

- Preparation of pellets using the raw product with a bit of water added. Those pellets are then crushed and sifted, in order to keep particles with an average diameter of 1 mm. This method allows an easier preparation of particles, but these remain fragile, and should be handled with care.

- Deposit a thin layer of the raw product in the porosity of particles, such as activated alumina. This method allows to generate particles with better mechanical behaviour, but these are more difficult to produce. Indeed, it is difficult to guarantee the quality (composition, thickness) of the deposit in the bottom of the pores.

The experimental program was performed using particles prepared according to the first method (crushed pellets). Modeling of the phenomena involved in reaction was based on shrinking core model with adhesive ashes. In this model, kinetics of manganese dioxide reduction by hydrogen can be written as:

$$r = k \exp(-E/RT) [H_2]^n$$

where kinetics parameters are k (kinetics factor), E (activation energy) and n (order of the reaction). This model is combined with a model describing the diffusion of hydrogen in ashes, and different relations in order to describe thermo-aeraulic phenomena involved in the system operation. Those model were implemented in the MITRHY code (ref 1). The point was then to determine the kinetics parameters (k, E and n) in order to complete the model. This was performed through various experiments, mainly in the CIGNE facility. CIGNE facility can be divided in 3 parts:

- gas preparation, allowing heating and water injection in the gas phase,
- the reaction zone is a fixed bed, that is a cylindrical vessel (diameter 30 mm, length between 35 mm and 140 mm) filled with particles of MnO_2/Ag_2O (diameter ~ 1 mm), maintained between two filters,
- gas analysis includes mass spectrometer (gas outlet) and infrared analysis (gas inlet and outlet).

After conditioning, the gas is flushed through the fixed bed, where hydrogen is converted into water. Hydrogen content of the gas phase is measured at the outlet of the reactor using mass spectrometer. Monitoring of the facility includes temperature (gas phase and solid) and gas flowrate. Figures 1 and 2 present the results of one test, including gas phase analysis and temperature of the fixed bed measurement during the test. Based on the experimental results, the following parameters have been calculated to describe the reaction kinetics:

- order of the reaction n = 1,
- activation energy E = 29428 J/mol H_2,
- kinetics factor k = 141,96 s^{-1}.

As an application, preliminary design calculation were performed, based on accident scenarii for ITER reactor. Two geometries have been investigated, based on fixed bed principle, i.e. a kind of “hydrogen conversion cartridge”, filled with MnO_2/Ag_2O particles, placed in the pipe between the Vacuum Vessel (VV) and the Vacuum Vessel Pressure Suppression System (VVPSS):

- Case 1 : one cartridge of the same diameter than the pipe (80 cm), filled with particles of MnO_2/Ag_2O.
- Case 2 : 200 cartridges of smaller diameter (10 cm) operating in parallel, filled with particles of MnO_2/Ag_2O.

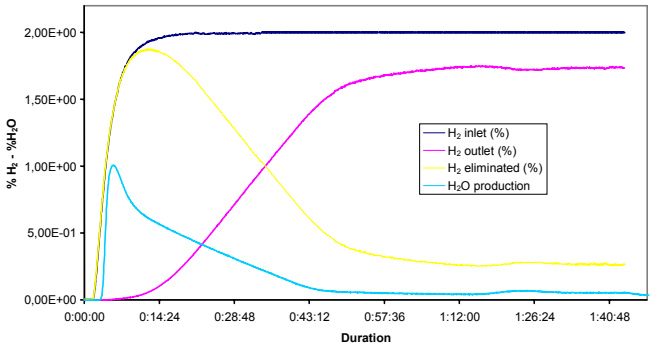

Figure 1 : CIGNE experimental results – Gas phase composition evolution

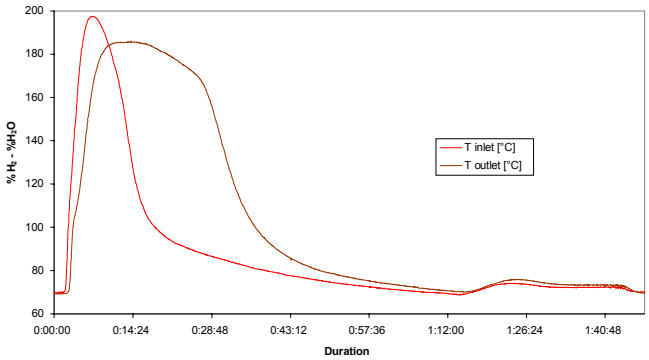

Figure 2 : CIGNE experimental results – Temperature evolution of the solid

In the first case, in order to avoid important pressure drop in the bed, it seems necessary to use large particles, actually small pebbles (diameter 10 mm), while the use of multiple smaller beds, with lower flow rate in each bed allows to use smaller particles (diam. 1mm) with larger specific surface.

Let's assume the following set of input data:

- hydrogen content in the gas phase (water vapor) = 5 %,
- total hydrogen content = 4,5 kg,
- evacuation time from VV to VVPS through the mitigation device = 500 s.

Results are then the following:

- Case 1 : 400 kg of solid allows the conversion of 0,935 kg of hydrogen.

- Case 2 : 263 kg of solid allows the conversion of 1,776 g of hydrogen.

This results shows the effect of the design on the device performance. However, final design is a compromise between efficiency of the process and technical feasibility, as the bundle of 200 reactors in parallel might be more complicated to implement on the future reactor.

Note : A final document is currently prepared, which will include all the results obtained during this study. It should be issued by the end of June 2003.

CONCLUSIONS

At the end of this study, the main results are the following:

- Hydrogen risk can be mitigated using a process based on metallic oxide reduction.

- A computer code was developed (MITRHY) to help for the design of a device based on this process.

- First application for ITER, based on accidental scenarii, shows the important effect of system design on its performance

Further work should include the study of other shaping of the product (for example, deposit on filtering cartridge), which could allow for easier implementation.

REFERENCES

[1] Mitigation of hydrogen risk using metallic oxide reduction - First model - NT DER/STPI/LPCP/99/086 J.C. ROBIN, R. MANSOURI.

REPORTS AND PUBLICATIONS

C. Maruéjouls , E. Bachellerie, C. Latgé , A. Laurent , J.M. Le Lann , J.C. Robin , S. Rosanvallon : Mitigation of the hydrogen risk in fusion facilities : first experimental results, Fusion engineering and design, SOFT 2002, Helsinki.

C. Maruéjouls , E. Bachellerie, C. Latgé , A. Laurent , J.M. Le Lann , J.C. Robin : Modelisation de la cinétique d'élimination de l'hydrogène en situation accidentelle dans les réacteurs de fusion thermonucléaires, SIMO 2002, Système d'Information Modélisation, Optimisation Commande en Génie des Procédés, 24-25 Octobre 2002 – Toulouse (France).

TASK LEADER

Jean-Charles ROBIN

DEN/CAD/DER/STR/LCEP
CEA Cadarache
13108 Saint Paul Lez Durance Cedex

Tél. : 33 4 42 25 75 20
Fax : 33 4 42 25 72 87

E-mail : jean-charles.robin@cea.fr